Translational Oncology
www.transonc.com

Volume 11 Number 4 August 2018 pp. 864–872 **864**

Ultrasound Doppler as an Imaging Modality for Selection of Murine 4T1 Breast Tumors for Combination Radiofrequency Hyperthermia and Chemotherapy

Martyna Krzykawska-Serda[*,†], Jason Chak-Shing Ho[*], Matthew J. Ware[*], Justin J. Law[*], Jared M. Newton[*,‡], Lam Nguyen[*], Mahdi Agha[*], Steven A. Curley[*,§] and Stuart J. Corr[*,¶,#,]**

[*]Baylor College of Medicine, Dept. of Surgery, Houston, TX, USA; [†]Jagiellonian University, Dept. Biophysics, Faculty of Biochemistry, Biophysics and Biotechnology, Krakow, Poland; [‡]Baylor College of Medicine, Interdepartmental Program in Translational Biology and Molecular Medicine, Houston, TX, USA; [§]Rice University, Dept. of Mechanical Engineering and Materials Science, Houston, TX, USA; [¶]University of Houston, Dept. of Biomedical Engineering, Houston, TX, USA; [#]Rice University, Dept. of Chemistry and Smalley-Curl Institute, Houston, TX, USA; [**]Swansea University, Medical School, Swansea, Wales, UK

Abstract

Noninvasive radiofrequency-induced (RF) hyperthermia has been shown to increase the perfusion of chemotherapeutics and nanomaterials through cancer tissue in ectopic and orthotopic murine tumor models. Additionally, mild hyperthermia (37°C-45°C) has previously shown a synergistic anticancer effect when used with standard-of-care chemotherapeutics such as gemcitabine and Abraxane. However, RF hyperthermia treatment schedules remain unoptimized, and the mechanisms of action of hyperthermia and how they change when treating various tumor phenotypes are poorly understood. Therefore, pretreatment screening of tumor phenotypes to identify key tumors that are predicted to respond more favorably to hyperthermia will provide useful mechanistic data and may improve therapeutic outcomes. Herein, we identify key biophysical tumor characteristics in order to predict the outcome of combinational RF and chemotherapy treatment. We demonstrate that ultrasound imaging using Doppler mode can be utilized to predict the response of combinational RF and chemotherapeutic therapy in a murine 4T1 breast cancer model.

Translational Oncology (2018) 11, 864–872

Introduction

One of the main challenges in cancer therapy is the accurate selection of a treatment schedule to fully optimize response in a particular patient. Information about the biophysical characteristics of a tumor before therapy can significantly increase therapeutic success and prevent patient overtreatment and possible adverse side effects from multitreatment regimes. We postulate that addition of hyperthermia treatment with selective ultrasound tumor prescreening can bring benefits to chemotherapy by triggering an increase in tumor perfusion and lead to enhanced uptake of chemotherapeutic drugs. Based on results presented in this paper, such an addition may be beneficial for specific groups of patients.

The effects of hyperthermia have been intensively studied in oncology since the 1970s and have been used to improve accumulation, localization, penetration, and subsequently the efficacy of numerous chemotherapeutic drugs [1,2,3]. Additionally, the synergistic effects between hyperthermia and chemotherapeutic

Address all correspondence to: Martyna Krzykawska-Serda, Dept. Biophysics, Faculty of Biochemistry, Biophysics and Biotechnology, Gronostajowa 7, 30-387 Krakow, Poland or Stuart J. Corr, Dept. of Surgery, Houston, TX, USA.
E-mail: martyna.krzykawska@uj.edu.pl
Received 16 February 2018; Revised 13 April 2018; Accepted 17 April 2018

1936-5233/18
https://doi.org/10.1016/j.tranon.2018.04.010

drugs, such as gemcitabine, appear promising [4]. In some cases, hyperthermia can also trigger the release of localized drugs that have already accumulated in the tumor tissue [5–7]. All of these served as a foundation for several hyperthermia clinical trials as a treatment modality in combination therapy (combined with radiotherapy and/or chemotherapy). The general conclusions from these clinical trials indicate a beneficial effect from hyperthermia treatment against cancer. Moreover, therapeutic outcome can be related not only to treatment protocol but also to the way in which heat is delivered to the target tissue.

Despite its suggested therapeutic promise, hyperthermia treatment is not always beneficial as its mechanism of action is still unclear, and its benefits are difficult to predict. A possible explanation is heterogeneity in tumor phenotypes and hence tumor response to hyperthermia. Pretreatment determination of predictive biophysical characteristics of a patient's tumor to select the best candidates for combination treatment represents a possible solution to these difficulties. In this context, tumor perfusion and the degree of intratumor vascularization are relevant factors in determining tumor response to hyperthermia. Ultrasound Doppler imaging can be used to accurately determine both of these biophysical characteristics of a tumor and hence provide a predictive element to tumor response due to hyperthermia therapy.

Ultrasound Doppler imaging allows the study of blood flow in vessels and provides a method to analyze functional tumor vasculature. Typically, tumor vessel structure is irregular in form with dilated, tortuous, and saccular microvessels with disorganized patterns of interconnection and branching [8], which lead to irregular or absent intratumoral blood flow regulation. Drug penetration into solid tumors is also impaired due to high interstitial fluid pressure (IFP) and pathological vasculature [9,10], which means that many compounds are not able to penetrate more than 40 to 50 μm from the vessel [11,12]. Furthermore, it has been shown that some normal tissue, like intestines, liver, or kidneys, can accumulate 10- to 20-fold more drug than the tumor tissue [13,14]. Due to these adverse intratumoral characteristics, it is difficult to obtain a homogeneous and disperse intratumoral drug distribution even with the possibility of the EPR effect playing a role and with the use of cancer-targeting modalities that are designed and used to possess increased tumor disposition and specificity. Therefore, tumors commonly develop multiple drug resistance and display deficient tumor responses to chemotherapy, meaning that therapeutic failure is inevitable [15].

Despite these challenges, we have previously shown that pathological tumor vasculature structure and permeability can be affected by hyperthermia leading to improved drug disposition in tumor tissue [16,17,18]. However, we believe that selecting specific tumor phenotypes to undergo hyperthermia therapy after pretreatment characterization of their biophysical features will allow a more predictable, reproducible, and efficacious therapeutic result.

Materials and Methods

Ethics Statement and General Experimental Conditions

All experiments were approved and performed in accordance with the Baylor College of Medicine Institutional Animal Care and Use Committee. Female Balb/c athymic FoxN1 nude mice were housed in standard temperature and lighting conditions with free access to food and water. All experiments (including heat delivery and imaging) were performed under isoflurane anesthesia (0.7%-2.5% isoflurane in medical air). After each anesthesia period (40-90 minutes), mice were monitored in a stable-heated recovery chamber. All intravenous (i.v.) injections were performed with 32G needles. All animals (n = 158) were euthanized with primary and secondary methods according to the protocol.

Tumor Model

4T1 breast cancer cells were cultured in RPMI-1640 media supplemented with 10% fetal bovine serum. Cells were maintained in a humidified atmosphere with 5% CO_2. A total of 10^5 4T1 cells suspended in base medium were injected into the left inguinal mammary gland to initiate orthotropic 4T1 breast tumors in Balb/c nude mice, as previously described by Pulaski and Ostrand-Rosenberg [19]. The rationale to use nude mice in the study was to avoid the shaving procedure, which can irritate the skin, affect microvasculature, and interfere with parameters under investigation. Additionally, presence of fur can disrupt temperature dosimetry, and hair can act as a thermal insulator, which may skew results. Treatment commenced 12 to 14 days after the injection of the cells and when tumors had reached approximately 250 mm^3.

Chemical Compounds

Gemcitabine (Gemzar; stock solution: 38 mg/ml)—The range of doses from 30 to 60 mg/kg BW was applied i.v. after reconstitution of stock solution in sterile saline solution (0.9% sodium chloride injection). Abraxane (stock: 100 mg paclitaxel, 900 mg albumin)—The range of dose from 15 to 30 mg/kg BW was applied i.v. after preparation of drug solution in sterile saline solution. Dosing was calculated with paclitaxel only. All drug solutions were used within 12 hours after preparation. A consistent injectable volume per mouse was maintained across all drug concentrations to avoid physiological changes related to the injection volume: 119 μl of gemcitabine solution for gemcitabine and 150 μl of Abraxane calculated for 25-g mice.

Hyperthermia Treatment

Two methods of delivering hyperthermia to target tissue were used: 1) noninvasive RF field hyperthermia and 2) contact-based heating using a warmed water balloon. Noninvasive RF field treatment of mice involved high-intensity (~90 kV/m) 13.56-MHz RF fields at various powers (0-1000 W) being administered to each mouse until a target temperature (37°C-43°C) was reached and maintained for 10 or 30 minutes depending on treatment group. Before the commencement of any procedures, temperature optimization was performed on a separate cohort of mice, which involved placing thermal probes intratumorally and calibrating a second method of measuring temperature which involved the use of an IR camera [18]. This also allowed the optimization of the experimental setup and the heating methods to obtain reproducible thermal doses in mice within and across various treatment groups. The contact-based heating (HC) technique delivered a thermal dose via the direct contact of the tumor surface with a water balloon connected to water circulator with an integrated thermocouple and feedback loop.

We have previously described, in detail, the differences and similarities of RF- and HC-based heating [18]. A "nonheat control group" (NHC) was also incorporated into the study design and relied on maintaining the core body temperature of each mouse to values similar to the core body temperature values of mice undergoing RF and HC treatment (32.5°C ± 2.5°C as measured via the insertion of a

rectal probe). The temperature of skin, tumor, and rectum was measured in each mouse using fiberoptic thermal probes and a real-time infrared camera (FLIR SC 6000, FLIR Systems, Inc., Boston, MA, USA). After the preliminary comparison of RF and HC and lack of difference in analyzed biological effects, the RF hyperthermia method of heat delivery was further investigated in a survival study as a safer and more uniform technique for heat delivery. For data analysis, all mice treated with hyperthermia were grouped into 3 categories: high (≥42°C), medium (39°C-41°C), and no (≤37°C) hyperthermia treatment.

Combined RF-Chemotherapy

Based on the literature [20,21,22–24] and our recent studies [16,17,18], the following combination treatment scheme (Supplementary Information, Figure S1) was applied with proper controls:

Hyperthermia Treatment Group

1) Abraxane injection i.v. with the range of doses: 15, 20, and 30 mg/kg BW. 2) RF treatment started 90 minutes after first chemo injection; during heating, tumor tissue was maintained at 41°C for 30 minutes with rectal temperature around 33°C. 3) Immediate gemcitabine i.v. injection after RF heating was done with the range of doses: 30, 40, and 60 mg/kg BW. This combinatory treatment was performed six times every 72 hours (Q3D6 protocol), resulting in 16 days of treatment time (day 1: first treatment day). The time interval between Abraxane and gemcitabine injection was 2 hours.

Chosen chemotherapy doses were categorized into three protocols to study the dose response relation: 1) 15 mg/kg of Abraxane followed with 30 mg/kg of gemcitabine, 2) 20 mg/kg of Abraxane + 40 mg/kg of gemcitabine, and 3) 30 mg/kg of Abraxane® + 60 mg/kg of gemcitabine. Each of the protocols was applied in the same time regimen and combined with the same RF treatment.

Controls Groups

1. Chemotherapy alone with the same dosages protocol as described above: Instead of RF treatment, the NHC protocol was applied (no tumor heating, maintaining the rectal temperature around 33°C);
2. RF alone: Instead of chemotherapy, a sterile saline solution was injected i.v. in the same time regimen and corresponding volume (150 μl for first injection, 119 μl for the second injection, for 25-mg mouse). RF treatment (tumor tissue maintained at 41°C for 30 minutes) was applied 90 minutes after the first saline injection;
3. Non-combined therapy–treated tumors: with sterile saline solution injection instead of chemotherapy administration and NHC protocol instead of RF heating.

Ultrasound Imaging

A Vevo 2100 ultrasonographic imager (VisualSonics, Toronto, Canada) with two transducers was used for noninvasive investigation of tumor tissue. The transducer MS-550S (wave frequency 32-56 MHz) was used to image in three different modes: 1) B mode, 2) Doppler mode, and 3) P/W mode. B mode was applied in standard VisualSonic presets for general abdominal imaging to determine morphological tumor characteristics (e.g., size, tumor position inside the gland). Doppler mode was used with very slow flow standard preset to determine the intratumoral functional vasculature network (PV) (vessels >30 μm with detectable blood flow). Imaging with 3D scaled image capture was used to reconstruct the 3D tumor image to determine tumor morphology and intratumoral large vessel structures. The P/W mode with fixed gate settings (and adjusted angle) was used to evaluate changes in blood flow, blood velocity, and the number of visible blood vessels per tumor.

The nonlinear contrast mode was used with an MS-250 transducer (13-24 MHz) with contrast agent (MicroMarker) to investigate tumor perfusion. To quantify tumor perfusion, a nontargeted MicroMarker ultrasound contrast agent (VisualSonic) was injected i.v. to enhance visualization of blood flow down to the capillary length scale (vessel detection up to 2-3 μm). The microbubbles, which consist of a phospholipid shell with perfluorobutene/nitrogen gas core, circulate freely through functional blood vessels. The bolus injection of the MicroMarker ultrasound contrast agent allows the microvasculature within the tumor to be studied by analysis of contrast uptake kinetics as well as percentage of tumor perfusion (PA) in tumor. The dynamic contrast enhanced imaging (DCE) methodology was applied to investigate the contrast influx into the tumor tissue [25], and a range of perfusion parameters was analyzed, e.g., peak enhancement (PE), time to peak (TTP), wash-in rate (WiR), and raise time (RT) [26]. The Vevo MicroMarker nontargeted contrast agent was used with a modified protocol, i.e., instead of the recommended catheter, a stretched PE tube was placed into the tail vain (estimated size 31G) as previously described [27]. The application of this type of catheter allowed us to perform whole sequence RF imaging with improved time efficiency and reproducibility, e.g., the contrast injection after RF was performed around 3 to 5 minutes after treatment was completed. To obtain high-quality DCE analysis, the physiological conditions of each mouse were established, and care was taken to maintain the same expiration rate, core body temperature, and heart rate during ultrasound imaging sessions for each mouse across each experimental group.

A syringe pump was used (KD Scientific KDS-210, Holliston, MA) for contrast injection and infusion. During contrast imaging, the microbubbles were injected as a single identical bolus (0.3-ml syringe: 60 μl per 15 seconds), followed by a 3-minute infusion (5 μl/min). The combination of bolus and infusion was experimentally optimized to obtain clear and reproducible data about the contrast agent influx into the tumor tissue (DCE analysis) and, next, after clear contrast PE, to obtain a stable signal time to collect 3D images of microbubble distribution (3D mode). All nondescribed imaging parameters and techniques were performed as recommended by the manufacturer [28]. Software Vevo LAB 1.7.1 (VisualSonic) was used to reconstruct and analyze all acquired images.

Histology

Immediately after resection, tissues were fixed with 10% formalin for 48 hours at room temperature. Tissues were histologically sectioned (2 μm) before standard hematoxylin and eosin staining was performed. Necrotic region and fat content quantification was carried out via manual segmentation of the necrotic or fat area using ImageJ software (NIH, USA) and presented as a percentage area fraction of the whole tumor area.

Experimental Design and Statistical Analysis

To design the experiment and randomize all treatment groups, the Design of Experiment module in Statistica12 software (StatSoft,

Tulsa, OK, USA) was used including full factorial design considerations (each variable, e.g., temperature, holding time, type of heating, drug dose, and treatment protocol, was randomized as an independent element before treatment). For statistical data processing, Statistica12 software was used to perform the various suitable types of statistical analyses, i.e., factorial analysis of variance (including Kruskal-Wallis, Kendall's, and median test), default set of distribution fitting, and linear fitting.

Results

To perform Kaplan-Meier analysis (Figure 1, *C* and *D*), the tumor kinetics were studied and the following survival criteria were chosen: a) not more than 20% loss of mouse weight in comparison to weight before the treatment and b) relative tumor volume (RTV) under 2.5, indicating the tumor growth was controlled. The RTV 2.5 was chosen based on tumor growth curves—in the majority of tumors, it is on the linear part of tumor growth just before the *plateau* or exponential growth starts or tumors lesions occurred. Usage of RTV instead of tumor volume allowed us to eliminate tumor heterogeneity as an imperative factor. Generally, a cutoff at 2.5 RTV provides independent tumor growth variability analysis (the slow- and fast-growing tumor can have the same RTV in days, which better describes the tumor response to therapy).

The combination of Abraxane (i.v.: 15, 20, 30 mg/kg BW) and gemcitabine (i.v.: 30, 40, 60 mg/kg BW) was used as described in the Materials and Methods section. We observed that the different chemotherapeutic drug dosages were not highly correlated with average (50%) survival (S. Figure 2): 7 days for control tumors vs. 26 days after A/G (30/60 mg/kg), 22 days after A/G (20/40 mg/kg), and 26 days after (15/30 mg/kg). Furthermore, the maximum animal lifetime was 11 days for untreated mice, 34 days for mice treated with A/G 30/60 mg/kg, 30 days when 20/40 mg/kg dosage was used, and 26 days for animals treated with the lowest chemotherapeutic drug dosage. Moreover, we noticed that hyperthermia improved the chemotherapy effectiveness only during and immediately after the treatment period (up to 20-24 days after the treatment started). For example, immediately after the Q3D6 treatment is completed, the increase of mouse survival after combination vs. monotherapy is 16% (the 30/60 dosage) (Figure 1, *A-D*). A few days after (up to 8 days posttreatment) the hyperthermia and chemotherapy treatment was completed, the difference between mice survival became insignificant ($P = .48$).

It is worth mentioning that hyperthermia could have a direct independent influence on cancer cell survival as implied by necrotic fraction data (Figure 1*E*) [29]. Analysis of tumor necrotic fraction (saline-treated mice with and without additional heating, $P = .04$) and our recent findings with RF treatment suggest that hyperthermia alone can increase cancer cell death. In the context of combined therapy, the antitumor effect is probably dominated by drugs, and potential hyperthermia-induced cancer cell death should be determined by more a precisely timed study. The *in vitro* experiment supports this finding [30].

During our research, we confirmed that hyperthermia treatment influences the immune system as presented in Figure 1*F*. The observed increase in neutrophils in circulating blood ($P < .01$) related to RF treatment can be additional benefits for hyperthermia combination therapy. The mechanism of immune system stimulation still remains unclear and remains under investigation.

The ultrasound imaging with Doppler mode visualizes vasculature vessels that are larger than 30 μm in diameter. We validated that the best protocol to image functional tumor vasculature with limited noise is the application of very slow flow VEVO2100 presets. During the analysis, we did not find any significant difference between contact-based heating (HC) technique and RF-induced hyperthermia on the fluid dynamics and percentage of functional vasculature (data not shown). Interestingly, we have previously suggested that RF-induced hyperthermia has enhanced effects on fluid dynamics in tumor tissue after heating in contrast to contact technique [18]. That is why all treatment protocols were classified as high thermal dose, medium thermal dose, and no hyperthermia treatment, as presented in Figure 2. The analysis of the percentage of vasculature area before any intervention (Figure 2*A*) allows us to divide all animals into two groups: 1) mice with hypovascularized tumors (PV < 2.95%) and 2) mice with a hypervasculaturized tumors, (PV > 2.95%). The significantly relevant increase of percentage of vasculature was only for animals with low PV before the medium-level hyperthermia treatment. It is worth noting that the median PV value in low vascularized tumors after mild hyperthermia is still smaller than PV in tumors with high vascularized group. Additionally, high hyperthermia treatment (≥42°C) induces no significant change of PV.

The tumor perfusion before and after hyperthermia treatment was investigated in independent experiments. We analyzed tumor perfusion maps (Figure 3, *A-D*) and normalized contrast kinetics (Figure 3, *E* and *F*). The contrast kinetics can be fitted and analyzed during dynamic-contrast enhancement analysis (DCE). As a result, a series of previously defined parameters was generated to describe tumor perfusion. The analysis of selected parameters of normalized contrast kinetics indicates that hyperthermia treatment is not able to change significantly the contrast agent kinetics and does not lead to change of total area of accumulated contrast intratumorally.

Discussion

The mechanism and biological effects of hyperthermia treatment on a tumor is dependent on the heating protocol, including the energy source, established temperature and the dissipation rate of the heat inside the target tissue, selectivity of heating, and the duration of hyperthermia treatment. Furthermore, the treatment outcome depends on the biophysical phenotype of the tumor being treated, such as tumor geometry, heat capacity, permittivity, and vascular network. The tumor vasculature plays an important role in tumor heat dissipation due to the well-known blood-heat sink effect [31]. Conversely, the intratumoral vascular networks influence drug disposition inside the tissue (if the drug is delivered via the intravenous route), and tumor perfusion also plays an important role.

It has been proposed for decades that increasing tumor temperature can lead to an increase of tissue perfusion and results in improved chemotherapeutic drug distribution. This hypothesis was tested by Shingleton [32], who used RF treatment to obtain tumor hyperthermia and observed a significantly greater level of C^{14}-labeled nitrogen mustard in the treated tissue. The mechanism was studied by the Song et al. who reported increased blood perfusion and tissue oxygenation in tumors treated with hyperthermia [33–35].

We designed our survival study to validate that RF hyperthermia treatment delivered into tissue with high precision and with stable 41°C intratumoral temperature can improve the survival of mice with breast cancer treated with chemotherapy. Previously, we showed our RF treatment procedure induced a significant increase of nanoparticles and fluorescent dye accumulation in a mouse breast cancer

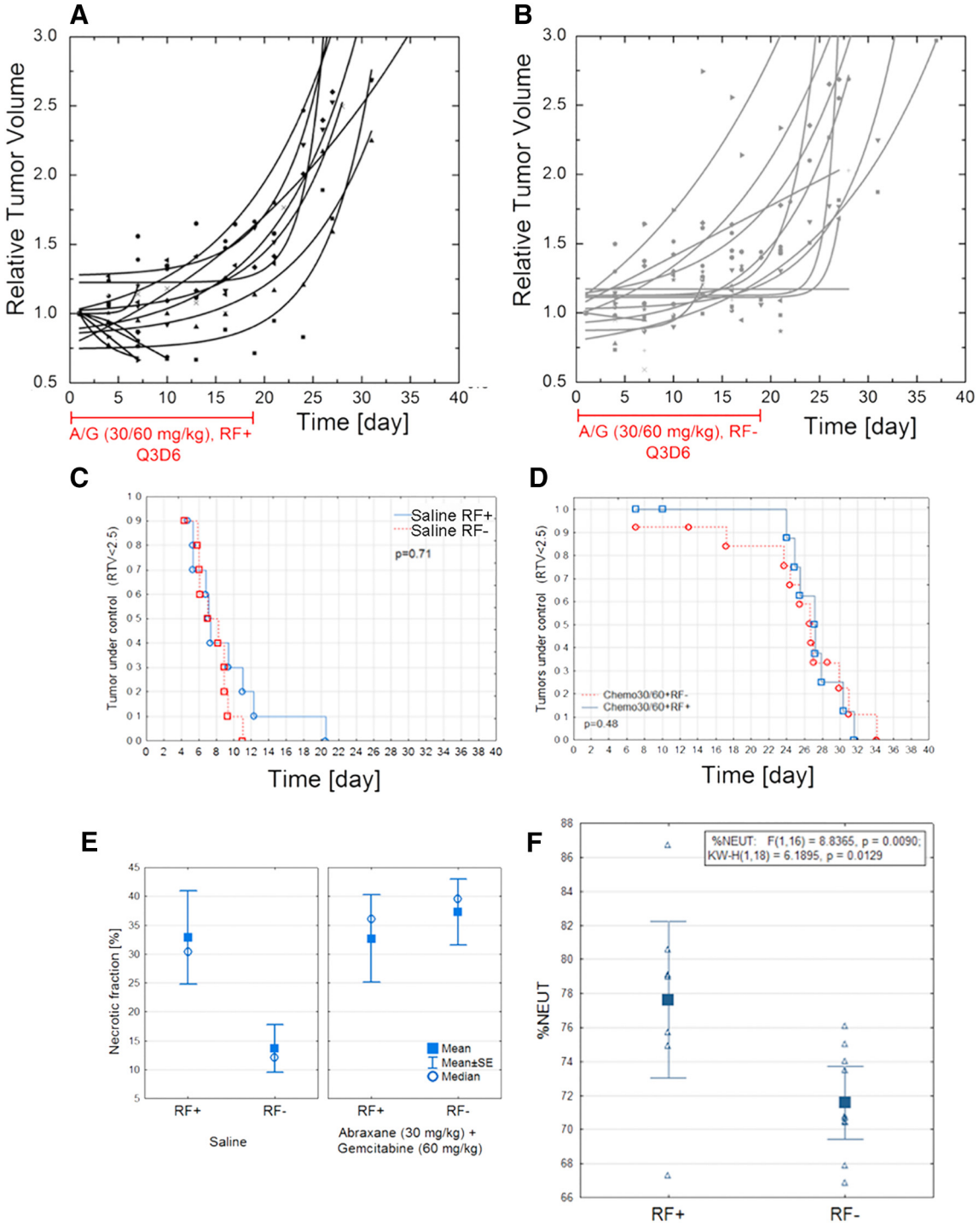

Figure 1. Combinational RF-chemotherapy treatment performed on Balb/c nude mice with orthotropic 4T1 mammary carcinoma. Relative tumor volume versus time for mice treated with chemotherapy regime with (A, $n = 13$) and without (B, $n = 13$) RF. Chemotherapy treatment was i.v. administration of 30 mg/kg Abraxane followed by 60 mg/kg gemcitabine, 2 hours apart. Kaplan-Mayer survival analysis for no-heat control groups with ($n = 10$) and without ($n = 10$) RF (C) compared to chemotherapy groups with ($n = 10$) and without ($n = 10$) RF (D). Note: Only mice with RTV < 2.5 and loss of animal body weight less than 20% were analyzed. (E) *Ex vivo* tumor analysis of necrotic fraction (%) versus treatment conditions. (F) Neutrophils (%) in mice blood treated with ($n = 8$) and without ($n = 10$) RF at end of observation time ($P = .01$). No chemotherapy was used in these groups.

model [16,18,36]. However, the results herein do not support the hypothesis that hyperthermia has a beneficial effect on survival of mice treated with chemotherapy. This can possibly be explained with the following: 1) the increase of drug accumulation is not present or is too small to affect the tumor growth; 2) the effect is too heterogeneous, and only a specific subpopulation of mice will benefit from combinatory treatment; and 3) the chemotherapy dosage is not optimal to study an effect on combinatory treatment. It is noteworthy that the doubling of the drug dosage (15 to 30 mg/kg BW of Abraxane and 30 to 60 mg/kg BW of gemcitabine) did not affect the

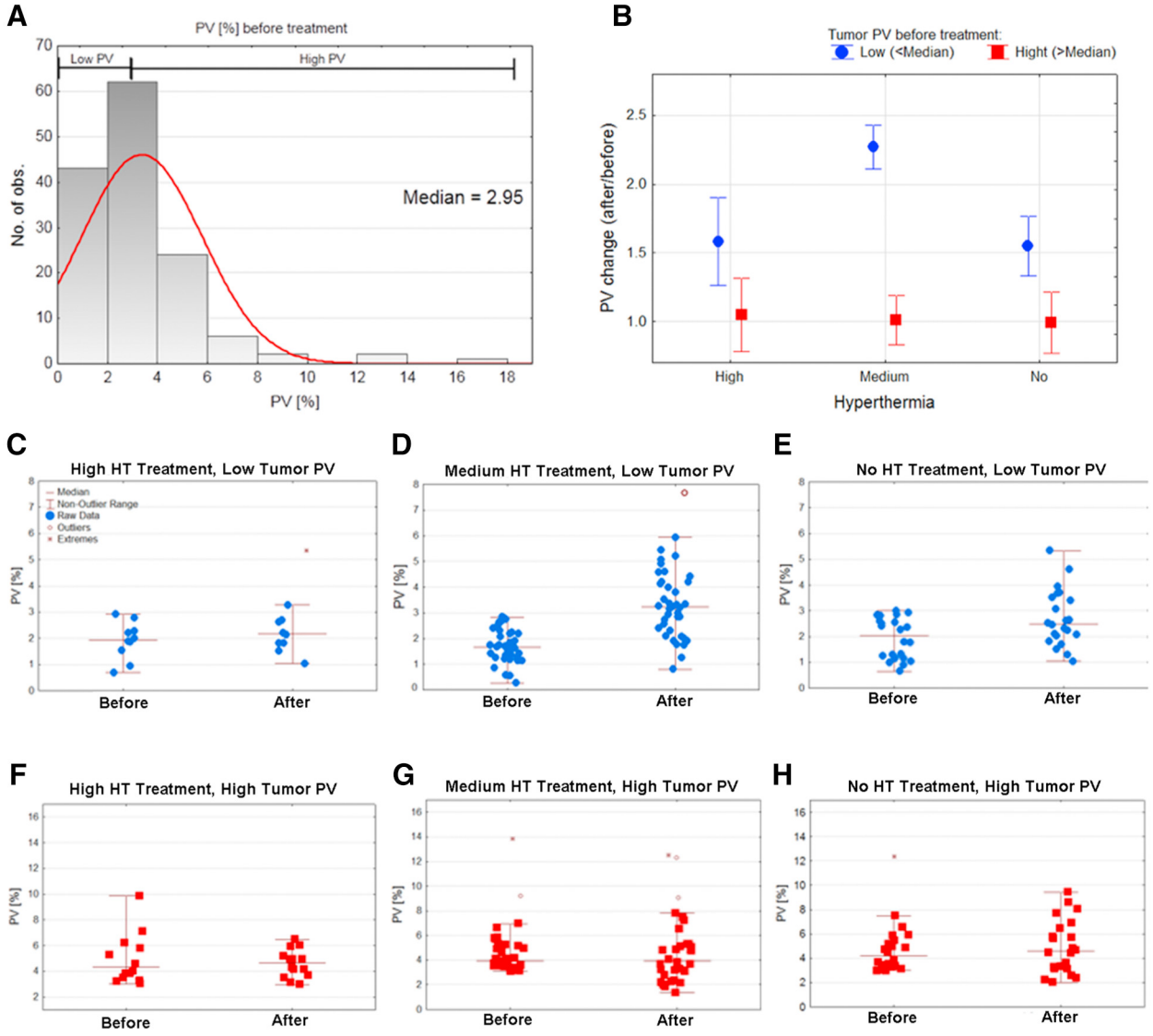

Figure 2. (A) Histogram of percentage of vasculature (PV) before the treatment ($n = 134$); (B) summary of PV change (ratio) in the result of high, medium, or no hyperthermia treatment ($n = 134$); (C-H) particular data points of PV in experimental conditions (blue: low tumor PV before treatment, red: high tumor PV before treatment). (C) High hyperthermia treatment, low tumor PV ($n = 9$); (D) medium hyperthermia treatment, low PV ($n = 38$); (E) no hyperthermia, low tumor PV ($n = 21$); (F) high hyperthermia treatment, high tumor PV ($n = 13$); (G) medium hyperthermia treatment, high tumor PV ($n = 32$); (H) no hyperthermia, high tumor PV ($n = 21$).

50% survival rate and only increased the maximum animal lifetime by 8 days. In this context, we calculated that approximately a 30% increase [18] in compound accumulation due to hyperthermia is still too little to affect the survival of mice with 4T1 tumors. In our previous study, we were able to obtain a significant increase of dye uptake after hyperthermia, which suggests that pretreatment predictive measures are warranted to target specific tumor phenotypes and hence improve therapeutic outcomes. We suggest that future survival studies should be designed with determination of tumor PV characteristics before therapy commences and treated as an independent factor in the randomization process.

Well-known benefits of ultrasound Doppler imaging are lack of invasiveness, great accessibility, low cost, and fast imaging of target tissue. Herein, we present data to support the hypothesis that after hyperthermia treatment the percentage of perfused tumor vasculature increases, but the effect is always in relation to established tumor vasculature networks before the intervention. We believe investigation of the tumor vascular network before treatment can provide significant information for therapy planning. The application of hyperthermia treatment for hypovascularized tumors before chemotherapy can increase drug accumulation and leads to better therapeutic effects. Lack of benefit of hyperthermia treatment on hypervascularized tumors can be explained by two reasons: 1) large and functional vessels can respond to increases in temperature by altering blood flow via vasodilation, and 2) a well-functioning vascular network cannot be improved by hyperthermia treatment because vessels are already efficiently maintaining blood flow (when trying to provide oxygen and nutrients to a permanently deficient tumor microenvironment).

Based on our results, in general, hyperthermia does not alter tumor perfusion (Figures 3 and 4). Tumor microvasculature is highly heterogeneous and often lacks normal mechanisms, e.g., paucity of endothelium or smooth muscle around the vessel. Hence, the response to hyperthermia on tumor microvessels can be difficult to

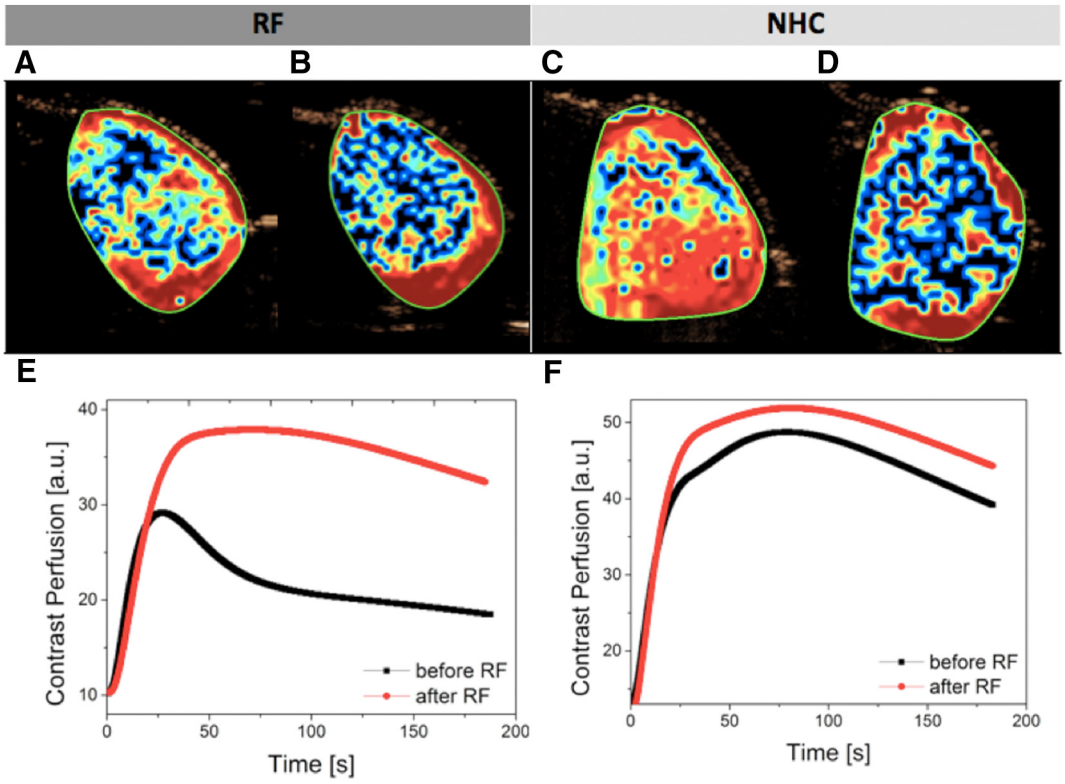

Figure 3. Examples of microbubble tumor perfusion maps with PE parameter presented with color scale (blue: low, red: high): (A) before RF and (B) after RF treatment, (C) before and (D) after NHC treatment. The normalized contrast uptake kinetic (fit) is presented before and after (E) RF and (F) NHC treatment of selected tumors (the curves described average kinetic for whole selected areas).

determine. Additionally, tumor perfusion imaging is much more sensitive to animal condition and quality of contrast injection than the degree of functional vasculature as established via imaging in Doppler mode. Despite these considerations, our results with contrast enhancement imaging do not confirm previous descriptions in the literature where hyperthermia influences tumor perfusion [34]. The contrast enhancement analysis did not shed light on possible drug uptake benefits after hyperthermia application (Figure 4).

Finally, we showed, in general, that medium thermal dose hyperthermia (39°C-41°C) is more efficient than higher thermal dose hyperthermia (>41°C) in increasing functional vasculature area (Figure 2). In our previous studies, we showed that temperatures higher than 42°C leads to reduction of blood flow in the vessels and can lead to vascular ablation [16]. Additionally, in the literature, the importance of tumor temperature was supported: tumors heated to 41.5°C are characterized by increased intratumoral pO_2, whereas 42.5°C leads to lack of significant difference in pO_2 in relation to untreated tumors, and 43.5°C leads to significant decline in tumoral pO_2 [33]. The biphasic effects of hyperthermia on tumor perfusion and vasculature were also explored by Vujaskovic et al. who showed that mild hyperthermia (41°C) can improve perfusion and oxygenation of treated tumors [37].

Conclusions

Adjunct hyperthermia with chemotherapy did not increase survival rates over the full time course of the experiment; however, it did improve the chemoefficacy at earlier stages during the treatment schedule. Selecting tumors with hypovascularity as determined by functional ultrasound Doppler imaging of blood flow for combinational hyperthermia/chemotherapy treatment may improve therapeutic outcomes. Tumors with low functional vasculature before the treatment displayed the greatest increase in functional vasculature after hyperthermia, which we believe can be beneficial for chemotherapy treatment. Tumor phenotypes with a preexisting significant functional vasculature will not benefit from adjuvant hyperthermia treatment. Tumor perfusion as established via contrast agent and contrast enhancement analysis did not provide a good biomarker for hyperthermia success as our analysis indicated that hyperthermia treatment is not able to significantly change intratumoral contrast agent kinetics and does not lead to an increase in accumulated contrast agent intratumorally. Finally, our findings confirm the hypothesis that larger thermal doses (>41°C) can induce adverse vessel effects, such as occlusion or destruction, and hence reduce drug disposition into the extravascular tumor microenvironment and do not use any significant increases in PV.

Acknowledgements

S. A. C., S. J. C., M. K. S., and M. J. W. acknowledge the financial support from Kanzius Cancer Research Foundation. J. M. N. acknowledges financial support from the National Institute of General Medical Sciences T32 predoctoral training grant (T32GM088129) and the National Institute of Dental & Craniofacial Research F31 NRSA training grant (F31DE026682) both of the National Institutes of Health. This content is solely the responsibility of the authors and does not necessarily represent the official views of the National Institutes of Health. The authors would like to acknowledge the Pathology and Histology Core, Baylor College of Medicine, Houston, TX, 77030 USA. We would like to

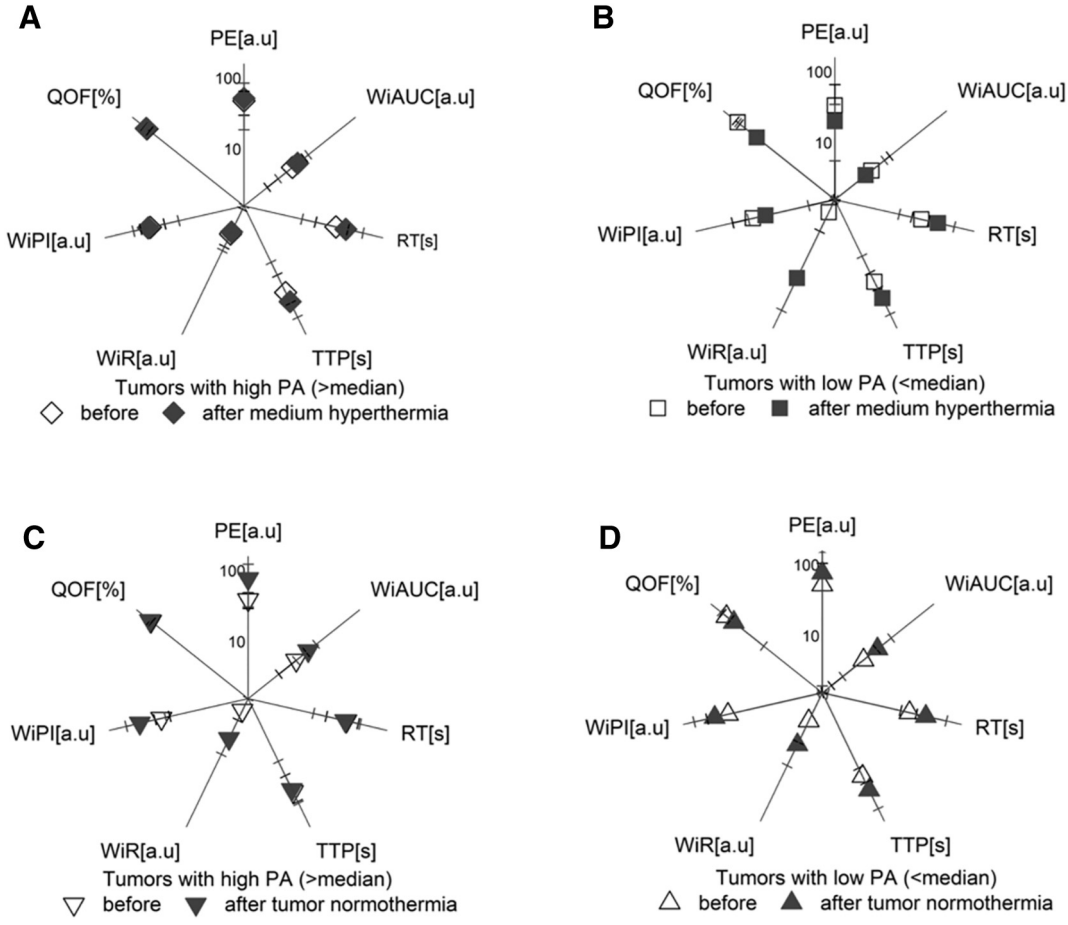

Figure 4. (A-D) Comparison of parameters of contrast kinetics before and after the treatment in selected experimental conditions. (A) High PA in tumors, medium hyperthermia ($n = 5$); (B) low PA in tumors, medium hyperthermia ($n = 5$); (C) high PA in tumors, normothermia ($n = 5$); (D) low PA in tumors, normothermia ($n = 4$). The DCE methodology was applied to investigate the contrast influx into the tumor tissue, and a range of perfusion parameters was analyzed, e.g., PE (peak enhancement), WiAUC [area under the curve (wash-in)], RT (raise time), TTP (time to peak), WiR (wash-in-rate), WiPI [wash-in perfusion index (WiAUC/RT)], QOF (quality of fit).

help prof. Martine J. Jager from Leiden University and prof. Martyna Elas for helpful discussions.

Author Contributions

The study was conceived by S. J. C., M. K. S., M. J. W., and S. A. C.; M. K. S., J. C. S. H., M. J. W., and S. J. C. designed the experiments. M. K .S., M. J. W., J. L., J. C. S. H., J. N., L. N., and M. A. performed the experiments. M. K. S. performed the data analysis. The manuscript was written by M. K. S. and edited by all authors before submission.

Competing Interests

The authors declare that they have no competing interests.

Appendix A. Supplementary data

Supplementary data to this article can be found online at https://doi.org/10.1016/j.tranon.2018.04.010.

References

[1] Frazier N and Ghandehari H (2015). Hyperthermia approaches for enhanced delivery of nanomedicines to solid tumors. *Biotechnol Bioeng* **112**(10), 1967–1983. https://doi.org/10.1002/bit.25653.

[2] Takahashi I, Emi Y, Hasuda S, Kakeji Y, Maehara Y, and Sugimachi K (2002). Clinical application of hyperthermia combined with anticancer drugs for the treatment of solid tumors. *Surgery* **131**, 78–84. https://doi.org/10.1067/msy.2002.119308.

[3] Gasselhuber A, Dreher MR, and Partanen A, et al (2012). Targeted drug delivery by high intensity focused ultrasound mediated hyperthermia combined with temperature-sensitive liposomes: Computational modelling and preliminary *in vivo* validation. *Int J Hyperthermia* **28**(4), 337–348. https://doi.org/10.3109/02656736.2012.677930.

[4] Vertrees RA, Das GC, and Popov VL, et al (2005). Synergistic interaction of hyperthermia and gemcitabine in lung cancer. *Cancer Biol Ther* **4**(10), 1144–1153. https://doi.org/10.4161/cbt.4.10.2074.

[5] Monsky WL, Kruskal JB, and Lukyanov AN, et al (2002). Radio-frequency ablation increases intratumoral liposomal doxorubicin accumulation in a rat breast tumor model. *Radiology* **224**(3), 823–829. https://doi.org/10.1148/radiol.2243011421.

[6] Kneidl B, Peller M, Winter G, Lindner LH, and Hossann M (2014). Thermosensitive liposomal drug delivery systems: state of the art review. *Int J Nanomedicine* **9**, 4387–4398. https://doi.org/10.2147/IJN.S49297.

[7] Perera RH, Solorio L, and Wu H, et al (2014). Nanobubble ultrasound contrast agents for enhanced delivery of thermal sensitizer to tumors undergoing radiofrequency ablation. *Pharm Res* **31**(6), 1407–1417. https://doi.org/10.1007/s11095-013-1100-x.

[8] Goel S, Duda DG, and Xu L, et al (2011). Normalization of the vasculature for treatment of cancer and other diseases. *Physiol Rev* **91**(3), 1071–1121. https://doi.org/10.1152/physrev.00038.2010.

[9] Heldin C-H, Rubin K, Pietras K, and Ostman A (2004). High interstitial fluid pressure—an obstacle in cancer therapy. *Nat Rev Cancer* **4**(10), 806–813. https://doi.org/10.1038/nrc1456.

[10] Provenzano PP, Cuevas C, Chang AE, Goel VK, Von Hoff DD, and Hingorani SR (2012). Enzymatic targeting of the stroma ablates physical barriers to treatment of pancreatic ductal adenocarcinoma. *Cancer Cell* **21**(3), 418–429. https://doi.org/10.1016/j.ccr.2012.01.007.

[11] Hambley TW (2009). Is anticancer drug development heading in the right direction? *Cancer Res* **69**(4), 1259–1261. https://doi.org/10.1158/0008-5472.CAN-08-3786.

[12] Minchinton AI and Tannock IF (2006). Drug penetration in solid tumours. *Nat Rev Cancer* **6**(8), 583–592. https://doi.org/10.1038/nrc1893.

[13] Bosslet K, Straub R, and Blumrich M, et al (1998). Elucidation of the mechanism enabling tumor selective prodrug monotherapy. *Cancer Res* **58**(6), 1195–1201.

[14] Chang DK, Lin CT, Wu CH, and Wu HC (2009). A novel peptide enhances therapeutic efficacy of liposomal anti-cancer drugs in mice models of human lung cancer. *PLoS One* **4**(1). https://doi.org/10.1371/journal.pone.0004171.

[15] Szakacs G, Paterson JK, and Ludwig JA, et al (2006). Targeting multidrug resistance in cancer. *Nat Rev Drug Discov* **5**(3), 219–234. https://doi.org/10.1038/nrd1984.

[16] Lapin NA, Krzykawska-Serda M, Ware MJ, Curley SA, and Corr SJ (2016). Intravital microscopy for evaluating tumor perfusion of nanoparticles exposed to non-invasive radiofrequency electric fields. *Cancer Nanotechnol* **7**(1), 5. https://doi.org/10.1186/s12645-016-0016-7.

[17] Corr SJ, Shamsudeen S, and Vergara LA, et al (2015). A new imaging platform for visualizing biological effects of non-invasive radiofrequency electric-field cancer hyperthermia. *PLoS One* **10**(8)e0136382. https://doi.org/10.1371/journal.pone.0136382.

[18] Ware MJ, Krzykawska-Serda M, and Chak-Shing Ho J, et al (2017). Optimizing non-invasive radiofrequency hyperthermia treatment for improving drug delivery in 4T1 mouse breast cancer model. *Sci Rep* **7**(March)43961. https://doi.org/10.1038/srep43961.

[19] Pulaski BA and Ostrand-Rosenberg S (2001). Mouse 4T1 breast tumor model. Current Protocols in Immunology. Hoboken, NJ, USA: John Wiley & Sons, Inc.; 2001. p. 1–16. https://doi.org/10.1002/0471142735.im2002s39.

[20] Zupi G, Scarsella M, and D'Angelo C, et al (2005). Potentiation of the antitumoral activity of gemcitabine and paclitaxel in combination on human breast cancer cells. *Cancer Biol Ther* **4**(8), 866–871 [doi:1895 [pii]].

[21] Von Hoff DD, Ervin T, and Arena FP, et al (2013). Increased survival in pancreatic cancer with nab-paclitaxel plus gemcitabine. *N Engl J Med* **369**(18), 1691–1703. https://doi.org/10.1056/NEJMoa1304369.

[22] Cividalli A, Mauro F, and Livdi E, et al (2000). Schedule dependent toxicity and efficacy of combined gemcitabine/paclitaxel treatment in mouse adenocarcinoma. *J Cancer Res Clin Oncol* **126**(8), 461–467. https://doi.org/10.1007/PL00021282.

[23] Colomer R, Llombart-Cussac A, and Lluch A, et al (2004). Biweekly paclitaxel plus gemcitabine in advanced breast cancer: phase II trial and predictive value of HER2 extracellular domain. *Ann Oncol* **15**(2), 201–206. https://doi.org/10.1093/annonc/mdh048.

[24] Frese KK, Neesse A, and Cook N, et al (2012). Nab-paclitaxel potentiates gemcitabine activity by reducing cytidine deaminase levels in a mouse model of pancreatic cancer. *Cancer Discov* **2**(3), 260–269. https://doi.org/10.1158/2159-8290.CD-11-0242.

[25] Cuenod CA and Balvay D (2013). Perfusion and vascular permeability: basic concepts and measurement in DCE-CT and DCE-MRI. *Diagn Interv Imaging* **94**(12), 1187–1204. https://doi.org/10.1016/j.diii.2013.10.010.

[26] VisualSonic. Application of the VevoCQ™ Software in Cancer Research: Application Note. URL: http://www.visualsonics.com/sites/default/files/AN_2100_Cb_VevoCQ_Cancer_Research_ver1.0.pdf.

[27] Haney CR, Parasca AD, and Fan X, et al (2009). Characterization of response to radiation mediated gene therapy by means of multimodality imaging. *Magn Reson Med* **62**(2), 348–356. https://doi.org/10.1002/mrm.22008.

[28] Visualsonics. Vevo MicroMarker™ Contrast Agent Kit: Contrast-Enhanced Applications Protocol and Information Booklet MicroMarker Kit Contents: Handling and Usage Instructions. URL: https://urresearch.rochester.edu/fileDownloadForInstitutionalItem.action?itemId=8123&itemFileId=16987.

[29] Ware MJ, Colbert K, Keshishian V, Ho J, Corr SJ, Curley SA, and Godin B (2016). Generation of homogenous three-dimensional pancreatic cancer cell spheroids using an improved hanging drop technique. *Tissue Eng Part C Methods* **22**(4), 312–321.

[30] Ware MJ, Tinger S, and Colbert KL, et al (2015). Radiofrequency treatment alters cancer cell phenotype. *Sci Rep* **5**(June)12083. https://doi.org/10.1038/srep12083.

[31] Fang Z, Zhang B, and Zhang W (2017). Current Solutions for the Heat-Sink Effect of Blood Vessels with Radiofrequency Ablation: A Review and Future Work. Singapore: Springer; 2017 113–122. https://doi.org/10.1007/978-981-10-6370-1_12.

[32] Shingleton WW (1962). Selective heating and cooling of tissue in cancer chemotherapy. *Ann Surg* **156**(3), 408–414http://www.ncbi.nlm.nih.gov/pmc/articles/PMC1466203/.

[33] Shakil A, Osborn JL, and Song CW (1999). Changes in oxygenation status and blood flow in a rat tumor model by mild temperature hyperthermia. *Int J Radiat Oncol Biol Phys* **43**(4), 859–865. https://doi.org/10.1016/S0360-3016(98)00516-1.

[34] Song CW (1984). Effect of local hyperthermia on blood flow and microenvironment: a review. *Cancer Res* **44**(10 Suppl), 4721s–4730s [http://www.ncbi.nlm.nih.gov/pubmed/6467226. Accessed March 7, 2014].

[35] Griffin RJ, Dings RPM, Jamshidi-Parsian A, and Song CW (2010). Mild temperature hyperthermia and radiation therapy: Role of tumour vascular thermotolerance and relevant physiological factors. *Int J Hyperthermia* **26**(3), 256–263. https://doi.org/10.3109/02656730903453546.

[36] Lapin NA, Krzykawska-Serda M, and Dilliard S, et al (2017). The effects of non-invasive radiofrequency electric field hyperthermia on biotransport and biodistribution of fluorescent [60]fullerene derivative in a murine orthotopic model of breast adenocarcinoma. *J Control Release* **260**, 92–99. https://doi.org/10.1016/j.jconrel.2017.05.022.

[37] Ujaskovic ZEV, Oulson JEANMP, and Askin AMAG, et al (2000). Temperature-dependent changes in physiologic parameters of spontaneous canine soft tissue sarcomas after combined radiotherapy and hyperthermia treatment. *Int J Radiat Oncol Biol Phys* **46**(1), 179–185.